Journal of Environmental Chemical Engineering 11 (2023) 110633

Contents lists available at ScienceDirect

Journal of Environmental Chemical Engineering

journal homepage: www.elsevier.com/locate/jece

Compact tubular carbon-based membrane bioreactors for the anaerobic decolorization of azo dyes

Mohammad Shaiful Alam Amin [a,b], Frank Stüber [a], Jaume Giralt [a], Agustí Fortuny [c], Azael Fabregat [a], Josep Font [a,*]

[a] Universitat Rovira i Virgili, Departament d'Enginyeria Química, Avinguda Països Catalans 26, 43007 Tarragona, Spain
[b] Shahjalal University of Science and Technology, Department of Chemical Engineering and Polymer Science, Sylhet 3114, Bangladesh
[c] Universitat Politècnica de Catalunya, Departament d'Enginyeria Química, EUPVG, Av. Víctor Balaguer, s/n, 08800, Vilanova i la Geltrú, Spain

ARTICLE INFO

Editor: <Xin Yang>

Keywords:
Anaerobic process
Azo dyes
Color removal
Tubular membrane

ABSTRACT

This research investigates a highly efficient compact tubular ceramic-supported carbon-based membrane reactor integrated with anaerobic biodegradation to decolorize the azo dyes. Two carbon-based membranes, produced using Matrimid 5218 polyimide and graphene oxide solutions, are evaluated for the comparative color removal of three structurally different azo dyes, Acid Orange 7 (AO7), Reactive Black 5 (RB5), and Direct Blue 71 (DB71). Based on FESEM microscopic images, the average pore size of the tubular ceramic-supported carbonized membrane (TCSCM) was approximately 25 nm, while for the tubular ceramic-supported graphene oxide membrane (TCSGOM), it was 12 nm. Additionally, TCSCM had a thinner layer at only 1.10 μm, while TCSGOM was slightly thicker at 2.11 μm. These features influenced the permeate flux of the membrane, in which the TCSGOM exhibited lower permeate flux (18.2 $L{\cdot}m^{-2}{\cdot}h^{-1}$) than the TCSCM (45.6 $L{\cdot}m^{-2}{\cdot}h^{-1}$). However, the anaerobic decolorization results indicated that the TCSGOM bioreactor (B-TCSGOM) was more efficient and effective at removing color from all dye solutions than the TCSCM bioreactor (B-TCSCM) over a wide range of feed concentrations. In both reactors, the highest decolorization was achieved at low feed concentration (50 $mg{\cdot}L^{-1}$), and removal was 94 % for AO7, 90 % for RB5, and 88 % for DB71 in B-TCSGOM, whereas 88 %, 85 %, and 69 %, respectively, in B-TCSCM. These suggest that the robust conductive nanoporous surface of B-TCSGOM makes it more effective at removing different azo dye solutions from wastewater.

1. Introduction

Textile industries are now one of the pillars of the contemporary economy. The manufacturing of clothes has increased due to the growth of the population, and as a consequence, the environmental impact associated with these processes has also increased [1]. Among the different textile manufacturing processes, the dyeing process is primarily responsible for water pollution as it uses a high amount of water to dissolve the azo dyes used to give color. This produces an enormous amount of wastewater, posing a severe environmental threat. Some azo dyes may be carcinogenic and cause several allergies [2]. Furthermore, it is also reported that they can affect neural, cardiac, and pulmonary systems and as well as cause reproductive problems [3]. The dyestuff wastewater treatment technologies have evolved over the years, and they can be divided into three broad categories: advanced oxidation processes (AOPs), biological treatments, and physicochemical methods.

The most common physicochemical treatments are ion exchange, precipitation, and adsorption [4]. In the case of adsorption processes, the dye molecules are adsorbed over the solid surface. In these cases, it is essential to point out that they are frequently expensive even if they are easy to operate. Moreover, their application is limited by the generation of toxic sludge and its high cost of adsorption disposal [5,6]. On the other hand, coagulation and flocculation need the addition of a reagent to produce the aggregation, which also increases the operational cost.

AOPs are treatment technologies that allow oxidizing the organic compounds present in wastewater by exploiting the reactivity of active species [7]. The literature has widely studied Fenton, Photo-Fenton, and ozonation processes [8–10] and shows the dye removal capabilities from wastewater. However, to optimize and enhance the performance of these processes, special attention to the process variables, such as pH, reagent dose, pollutant concentration, temperature, UV source, etc., is needed [11]. In addition, it may produce secondary pollutants requiring

* Corresponding author.
E-mail address: jose.font@urv.cat (J. Font).

https://doi.org/10.1016/j.jece.2023.110633
Received 20 April 2023; Received in revised form 17 July 2023; Accepted 23 July 2023
Available online 24 July 2023

to undergo furthermore treatment. Thus, the high operating cost (high amount of acid and/or base and energy consumption) makes it difficult to be applied on an industrial scale [12].

Biological treatments are processes in which organic contaminants act as nutrients for microorganisms [13]. These methods are typically employed in wastewater treatment plants because of their capability of removing suspended particles and color as well as keeping the biochemical oxygen demand at the desired level. These treatments can be aerobic or anaerobic, i.e., operating with or without oxygen. Compared to aerobic dye removal, anaerobic decolorization of azo dyes is an environmentally acceptable way of treating dyestuff molecules. Effluent is made safe for disposal or reuse as color intensity is lowered and potentially harmful compounds are removed or broken down [4]. Though the process is less expensive than competing methods, the process is relatively slow due to the inadequate electron transfer rate mechanism. Thus, it is economically challenging to remove such contaminants in a continuous mode [14].

In recent years, membrane technology has gained the attention of researchers and has become a potential wastewater treatment process. Membrane units allow for overcoming some of the mentioned limitations: the smaller size of the equipment, less energy consumption, and low capital cost. Moreover, it may not use chemicals, thus being an environmentally-friendly and accessible alternative [15]. However, the lifetime of the membranes is short, and their surface is exposed to readily fouling.

A combination of different methods can obtain a better azo dye removal process. Among all the possible alternatives, coupling membrane technology and anaerobic digestion is an effective solution, giving rise to anaerobic membrane bioreactor systems [16–19]. This technique minimized the major obstacle of the conventional anaerobic decolorization process, which was the slow transfer of electrons between microorganisms and dye molecules (to the azo, hydrogen, and other bonds) that ultimately hinders biodegradability, and prolongs the residence time [17]. In these works, the authors used flat ceramic supports to prepare a carbon-based membrane that usually showed superior chemical and thermal resistance, making them suitable for anaerobic biodecolorization of azo and other dyes. It supports microorganisms to grow biofilm, pollutant immobilization and enhances electron transfer between bacteria and dye molecules. This triple role is essential in achieving efficient biodegradation of azo dyes under anaerobic conditions. Though the color removal was comparatively high enough, it may be insufficient for the large-scale application because of the low permeate flow. However, it can be overcome using more compact geometries, for instance, tubular membranes, as they present a greater surface-to-volume ratio, higher mechanical strength as well as better resistance to high crossflow velocities.

Therefore, the main objective of this work is to synthesize tubular ceramic-supported carbon-based membranes. As the first option, one of the membranes is synthesized by the carbonization of Matrimid 5218 polyimide solution. In turn, the other tubular membrane is made of graphene oxide by vacuum-assisted filtration of an exfoliated graphene oxide solution. The novelty of this study is the integration of tubular carbon-based membranes with the anaerobic biodegradation method to successfully remove azo dye from dye-containing wastewater, which is the first time reported to the best of our knowledge. Throughout the experiments, both tubular membrane bioreactors were investigated for the anaerobic decolorization of monoazo Acid Orange 7 (AO7), diazo Reactive Black 5 (RB5), and triazo Direct Blue 71 (DB71) dye solutions at various feed concentrations.

2. Experimental

2.1. Preparation of tubular ceramic-supported carbon membrane

Ultrafiltration tubular ceramic membranes (inner diameter: 3 mm, length: 250 mm, molecular weight cut-off: 50 kg·mol^{-1}, TAMI Industries, France) served as the tubular ceramic support (TCS) for depositing the carbon layer. The tubular ceramic-supported carbonized membrane (TCSCM) used 10 % wt. Matrimid 5218 (Huntsman Advanced Materials, The Woodlands, TX, USA) as membrane precursor that was prepared by dissolving the desired portion of polymeric precursors in NMP (1-methyl-2-pyrrolidone, Sigma Aldrich, ref. 328634, Spain). Fig. 1 illustrates the schematic diagram of the tubular ceramic-supported carbon-based membrane fabrication. In TCSCM, the polymeric layer inside the TCS was formed by flowing (up-flow) of matrimid solution, in-out, through the membrane, continuously for 60 min (as shown in Fig. 1a). The membrane was subsequently dried for one hour and repeated the coating process three times. Afterward, the coated membrane was dried for 24 h, and then the carbon membrane was created using the carbonization of the coated membrane at 800 °C in an inert atmosphere [16].

For the other carbon-based membrane, tubular ceramic-supported graphene oxide membrane (TCSGOM), the membrane precursor was exfoliated graphene oxide (GO) solution, which was generated using a modified Hummer method [20] starting from 20 μm of pristine graphite powder (Sigma Aldrich, ref. 282863, Spain). The porous graphene oxide layer in the TCSGOM was formed by vacuum-assisted filtration, in-out, of 3–5 mL of 1 mg·mL^{-1} homogenous GO solution through the TCS in a filtration cell (MEMBRALOX® ET1-070, Pall Corporation, Bazet, France). Following filtration for thirty minutes, the membrane was first dried at 80 °C for 24 h and then at 100 °C for 72 h to obtain a stable and robust TCSGOM.

2.2. Experimental set-up for anaerobic biodegradation

Fig. 2 illustrates the experimental set-up for the comparative anaerobic biodecolorization of azo dyes using both carbon-based membrane bioreactors (B-TCSCM and B-TCSGOM). The monoazo AO7 (ACROS Organics, ref. 416561000, Spain) was used as the first target to test. Afterward, the second and third were diazo RB5 (Sigma Aldrich, ref. 306452, Spain) and triazo DB71 (Sigma Aldrich, ref. 212407, Spain) solutions. The specific dye, Sodium Acetate (Sigma Aldrich, ref. 110191, Spain), and basal medium were combined to form the artificial feed solution in each experiment [21]. The basal media, formed by six sets of microelements (mg·L^{-1}), contained i) $MnSO_4{\cdot}H_2O$ (0.16), $CuSO_4{\cdot}5\ H_2O$ (0.285), $ZnSO_4{\cdot}7\ H_2O$ (0.46), $CoCl_2{\cdot}6\ H_2O$ (0.26), $(NH_4)_6Mo_7O_{24}$ (0.285), ii) K_2HPO_4 (21.75), $Na_2HPO_4{\cdot}2\ H_2O$ (33.40), KH_2PO_4 (8.50), iii) $FeCl_3{\cdot}6\ H_2O$ (29.06), iv) $CaCl_2$ (13.48) v) $MgSO_4{\cdot}7\ H_2O$ (15.2), and vi) NH_4Cl (190.90). All chemicals were obtained from Sigma Aldrich (Spain) and dissolved in Milli-Q water (Millipore Milli-Q system, Molsheim, France). The source of the anaerobic sludge was the untreated aerobic secondary sludge from recirculation that was received from a wastewater treatment plant serving the municipality of Reus, Spain. At first, the aerobic sludge was stored in an anaerobic environment for one week so that it might undergo partial digestion. After that, the sludge was passed through a filter made of glass wool, and then it was allowed to run through a filter made of paper to obtain a single cell or spore. This monocellular sludge was once again stored in anaerobic conditions for further application.

For the anaerobic biodecolorization of azo dyes, the TCSCM and TCSGOM membranes were inserted in the appropriate filtration cells, which also perform as bioreactors. Following, 5 mL of anaerobic sludge was injected inside the tubular carbon-based membranes. In the end, the bioreactor is properly sealed so that there is no risk of leakage, contamination, or the presence of oxygen. The continuous flow of pressurized nitrogen gas (purity >99.99 %, Linde, Spain) into the feed tank enables the feed solution to be pumped to the bioreactor. It also contributes to establishing an anaerobic condition in the feed tank. The gas flow was adjusted throughout the operation to set the transmembrane pressure (TMP) and simultaneously provide a negative redox potential to ensure suitable conditions for the decolorization [22]. A refrigerator and incubator (Selecta Group SA, Madrid, Spain) were used

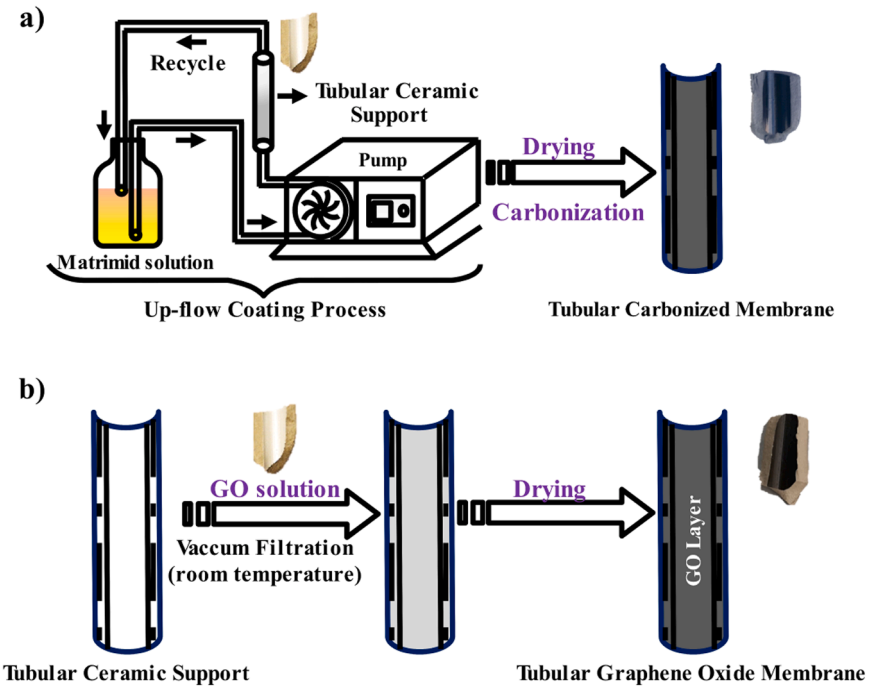

Fig. 1. Fabrication process of the Tubular Ceramic-supported Carbon-based Membranes a) Tubular ceramic-supported carbonized membrane (TCSCM) b) Tubular ceramic-supported graphene oxide membrane (TCSGOM).

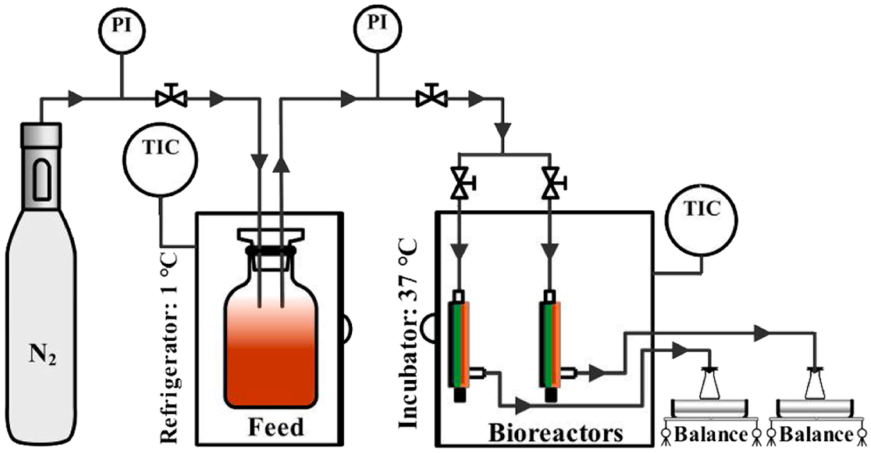

Fig. 2. Experimental set-up for anaerobic decolorization of dye molecules by TCSCM and TCSGOM.

to control the temperature of the feed solution and anaerobic bioreactors. Therefore, the temperature of the feed tank and bioreactor was maintained at 1 ± 1 ºC and 37 ± 1 °C, respectively, to prevent the uncontrolled growth of microorganisms, avoid the consumption of sodium acetate outside the bioreactor and thus attain the maximum color removal [23,24]. The compact tubular membrane bioreactors were operated in a dead-end filtration mode under a constant permeate flux of 0.10 $L{\cdot}m^{-2}{\cdot}h^{-1}$. Quickly, the biofilm formed over the membrane carbon layer and adapted to dye, carbon sources, and basal medium. Thus, both anaerobic biodegradation and membrane filtration occurred simultaneously in this novel tubular carbon-based membrane bioreactor. Throughout the operation, the permeate flow was constantly measured to keep the constant flux filtration, and two membrane bioreactors operated at once to compare the anaerobic bioreduction of azo dyes.

2.3. Membrane characterization

The chemical structures of the tubular carbon membranes were analyzed using the Fourier Transform Infrared (FT-IR) Spectrophotometer (FT/IR-6700, JASCO, Tokyo, Japan). In addition, X-ray diffraction (XRD) was performed with a Bruker-AXS D8-Discover diffractometer (Bruker-AXS, Germany; operated under 40 kV and 40 mA to generate 1.54056 Å CuK_{α} radiation) to identify the phase purity and crystallinity of the synthesized tubular carbon-based membranes. Further, the deposited carbon layer pore size, thickness, and microelements were examined by a combined Focused Ion Beam-Scanning Electron Microscope (FIB-SEM, Scios 2 Dual Beam, Thermo Scientific, MA USA).

2.4. Analytical methods

Membrane flux, pure water permeance (PWP), and hydraulic resistance were used to determine the filtration performance, which was

computed using Eqs. (1–3),

$$J = \frac{\Delta V}{\Delta t}\cdot\frac{1}{A} \quad (1)$$

$$\text{PWP} = \frac{J}{\Delta P} \quad (2)$$

$$H_R = \frac{\Delta P}{\mu}\cdot\frac{1}{J} \quad (3)$$

where J denotes the permeate flux through the tubular membrane ($L{\cdot}m^{-2}{\cdot}h^{-1}$), V is the permeate volume that passes through the membrane (L), t is the filtration time (h), A the membrane filtration area (m^2), H_R is the hydraulic resistance (m^{-1}), ΔP is the transmembrane pressure (bar), and μ is the viscosity of water (Pa·s).

A UV/VIS4000n Spectrophotometer (DINKO Instruments, Spain) was used to quantify the decolorization (D) that occurred during the anaerobic bioreduction of the azo dye, which was then calculated using Eq. (4).

$$D\,(\%) = \frac{A_o - A}{A_o} \times 100 \quad (4)$$

A_o and A being the absorbance of feed and permeate liquid, i.e., before and after the biodegradation process.

3. Results and discussion

3.1. Characterization of tubular ceramic-supported carbon membranes

The functional groups of the TCSCM and TCSGOM were characterized by FTIR and are depicted in Fig. 3(a-b). The peaks at 1717.23 cm^{-1} in TCSGOM (Fig. 3a) are attributable to the C═O group, whereas the peak at 1601.23 cm^{-1} owns to the presence of the sp^2 bond for the aromatic C═C skeletal vibrations. A moderate peak shows the stretching vibrations of the C-OH bond at 1417.23 cm^{-1}. Another distinctive signal at 1039.78 cm^{-1} corresponds to the C-O-C groups, demonstrating that pristine graphite has been completely oxidized [25]. In Fig. 3b, the typical FTIR spectra of the polymeric membrane, i.e., before the carbonization, shows at 2955.12, 1713.23, 1497.31, 1368.98, 1090.01, and 712.16 cm^{-1}, the stretch of the methyl group (C-H), C═O, C═C, C-N-C axial, C-N-C transverse, and C-H (monosubstituted of benzene) groups, respectively [26,27]. After carbonization, the spectrum does not show apparent peaks from 3600 to 600 cm^{-1}. This proves that the polymeric precursor completely decomposes and breaks its chemical structure during carbonization [26,28].

XRD diffractograms of ceramic support (TCS) and carbon-based membranes (TCSCM, and TCSGOM) are displayed stack-by-stack in Fig. 4, which were measured under identical operating conditions. When compared, all of the samples have the same distinctive peaks at 2θ= 16, 28, 43, 35, 54, and 59°, which are associated with the rutile form of TiO_2 [17]. Tubular ceramic-supported carbonized membrane (TCSCM) have been shown to contain graphitized carbon, as evidenced by peaks at 2θ= 25.9°, while in TCSGOM, instead of this one, identical peaks at 2θ= 10° indicate that the GO crystal plane (001) has been formed [18]. In addition, this TCSGOM diffractogram represents the complete oxidation of all graphite to graphene oxide.

Fig. 5(a-d) shows the microstructural analysis of the two carbon-based membranes, taken in the top surface and the cross-section. Fig. 5(a-b) suggests a smooth and defect-free surface for both tubular ceramic-supported carbonized membrane (TCSCM) and tubular ceramic-supported graphene-oxide membrane (TCSGOM), although indeed looks different in pore size. The average pore size of TCSCM was estimated to be 25 nm, while it was 12 nm for TCSGOM. Consistent with previous research, the current results indicate that the pore size of a TCSGOM is smaller than that of a TCSCM. On the other hand, opposite results were found for the carbon layer thickness, which was deposited on the top of the ceramic support. The thickness was measured as 1.10 and 2.11 μm, respectively, for TCSCM and TCSGOM. The carbonization of TCSCM at a high temperature resulted in forming of a thinner carbon layer than that of TCSGOM [29]. However, the layer was asymmetric, tightly packed, and strongly attached to the tubular support in both cases.

3.2. Permeate flux and hydraulic resistance of the tubular carbon-based membranes

The TCSCM and TCSGOM membrane flux, pure water permeance (PWP), and hydraulic resistance (H_R) were examined to evaluate the effect of the carbon layers deposited over the tubular ceramic supports. Three filtration tests over either TCS, TCSCM, or TCSGOM were conducted within a range of transmembrane pressures (TMP). As shown in Fig. 6, the TCS, due to the absence of any additional carbonaceous layer, exhibited the highest permeate flux (197.4 $L{\cdot}m^{-2}{\cdot}h^{-1}$) as well as water permeance (247.3 $L{\cdot}m^{-2}{\cdot}h^{-1}{\cdot}bar^{-1}$) at the TMP of 0.80 bar. With respect to the other two, the TCSGOM owned the lowest permeate flux, 18.2 $L{\cdot}m^{-2}{\cdot}h^{-1}$, and PWP, 22.8 $L{\cdot}m^{-2}{\cdot}h^{-1}{\cdot}bar^{-1}$, which is 90 % and 60 %, respectively, lower than the TCS and TCSCM (Flux: 45.6 $L{\cdot}m^{-2}{\cdot}h^{-1}$

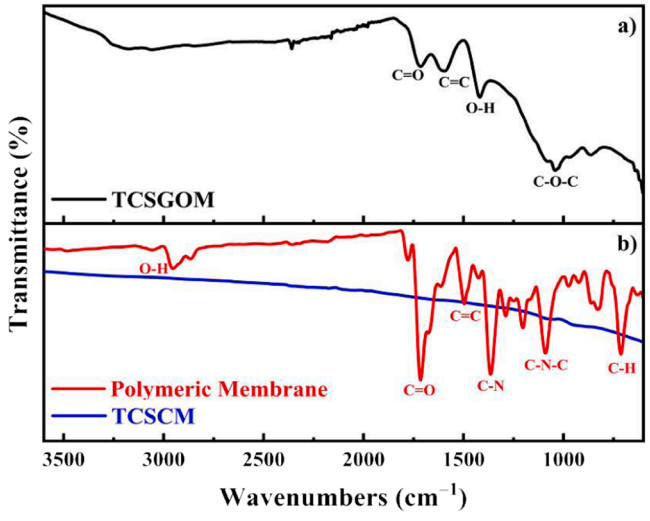

Fig. 3. FTIR analysis of the a) TCSGOM and b) polymeric precursor membrane and TCSCM (TCSCM: 10 % wt. Matrimid and TCSGOM: 1 $mg{\cdot}L^{-1}$ GO solution).

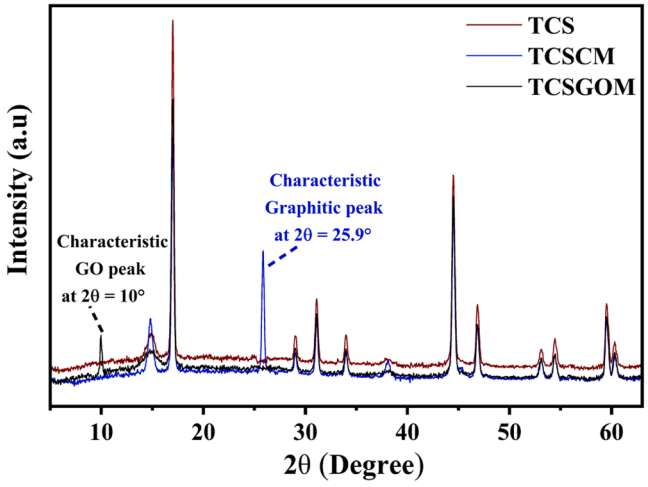

Fig. 4. X-ray diffractogram of the tubular ceramic support (TCS) and the tubular ceramic-supported carbon-based membranes (TCSCM: 10 % wt. Matrimid and TCSGOM: 1 $mg{\cdot}L^{-1}$ GO solution).

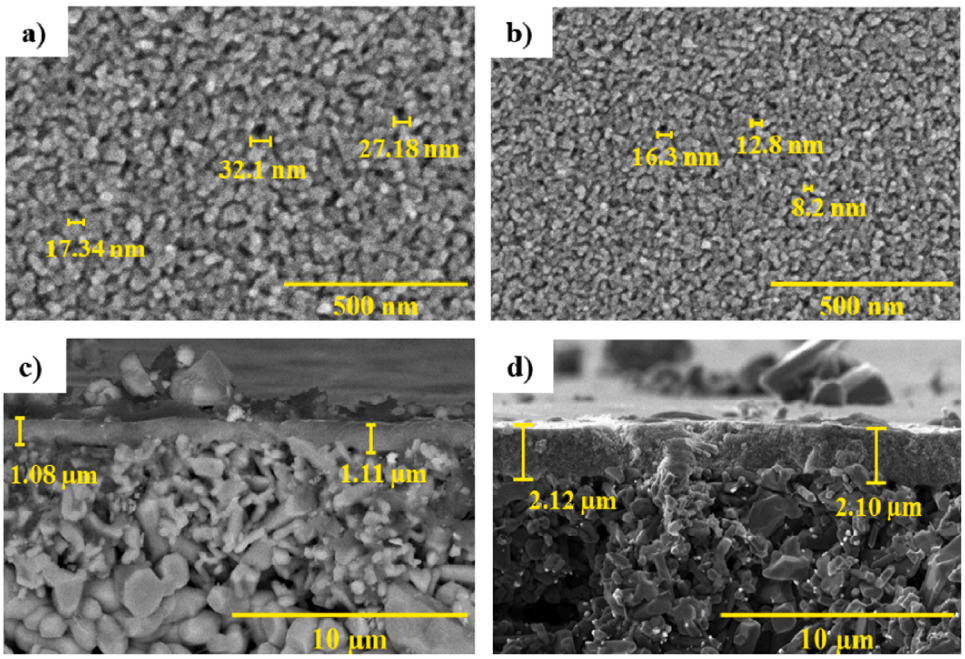

Fig. 5. FESEM microscopy images a-b) the surface of TCSCM and TCSGOM, and c-d) the cross-section of TCSCM and TCSGOM (TCSCM: 10 % wt. Matrimid and TCSGOM: 1 mg·L^{-1} GO solution).

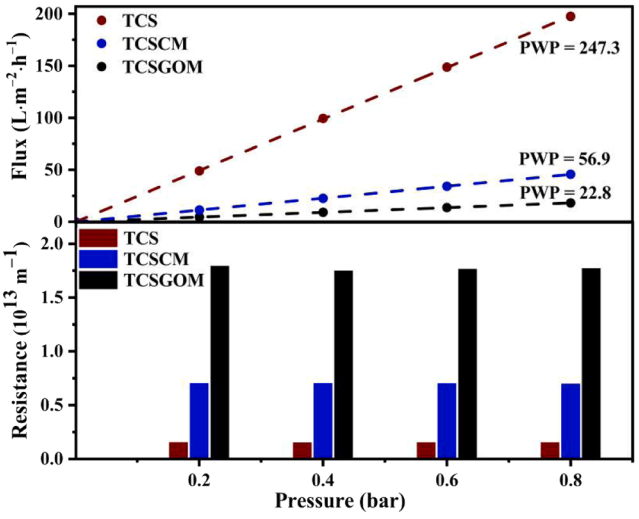

Fig. 6. Variation of membrane flux, water permeance, and hydraulic resistance as a function of TMP for TCS, TCSCM, and TCSGOM.

and PWP: 56.9 L·m^{-2}·h^{-1}·bar^{-1}). The variation of the hydraulic resistance was depicted in Fig. 6, too, as a bar chart. Following the permeances, the TCSGOM displayed the highest hydraulic resistance (1.78 ± 0.01 ×10^{13} m^{-1}), while TCS had the lowest (1.62 ± 0.01 ×10^{12} m^{-1}).

Compared to TCS, the decrease in membrane flux of TCSCM and TCSGOM is predominantly due to the deposition of an additional carbon layer on the ceramic support inner surface. Again, the distinction of flux between these two carbon-based membranes depends on the thickness and pore size of the carbon layers covering the membrane surface. As shown in the FESEM images, Fig. 5(a-d), the carbon layer thickness of TCSCM was thinner than that of TCSGOM. This occurred due to the presence of NMP in the highly viscous Matrimid solution, which evaporates slowly during the carbonization at a high temperature causing the membrane pores to be larger in size but thinner than the carbon layer [30]. On the other hand, the exfoliated GO solution partially penetrated the ceramic support (GO-TiO_2 region) and slightly blocked the support pores. Then, it continues growing to form single or several graphene oxide layers over the tubular support. Amin et al. [16,17] also observed a similar trend over the flat CSCM that exhibited higher filtration flux and permeance than flat CSGOM. Owing to the little porous and thick graphene oxide layer, TCSGOM demonstrated higher hydraulic resistance than the others.

3.3. Role of the membrane type on anaerobic decolorization of dyes

Carbon-based membranes (both TCSCM and TCSGOM) and ceramic support (TCS) were examined to assess the color removal from the model azo dye solution. The feed solution contained 50 mg·L^{-1} of Acid Orange 7 (AO7), and the anaerobic biodegradation was carried out under one-pass dead-end filtration mode at constant permeate flux (0.10 L·m^{-2}·h^{-1}). The three bioreactors operated with TCS, TCSCM, and TCSGOM are henceforth referred to as B-TCS, B-TCSCM, and B-TCSGOM, respectively; in turn, another reactor consisting of only TCS was performed without microorganisms labeled as R-TCS. As illustrated in Fig. 7, AO7 biodecolorization drastically depends on the presence of the carbon layer and microorganisms. Compared to R-TCS and B-TCS, both compact carbon-based membrane bioreactors (B-TCSCM and B-TCSGOM) demonstrated stable color removal over ten-day periods and beyond, in which B-TCSGOM was able to decolorize 97 % of AO7 monoazo dye at the highest whilst B-TCSCM stabilized at around 90 %.

Just at starting, instantaneously, all the reactors showed good dye removal efficiency. Still, after 12 h of operation, the decolorization abruptly dropped from 70 % to 33 % for B-TCS and 65–15 % for R-TCS. Finally, after two days, both R-TCS and B-TCS, the bioreactors exhibited nil capacity to remove any color. In the initial phase of decolorization, the dye was mostly adsorbed by the membrane surface. However, this process cannot be considered as the true decolorization process. The effectiveness of removing color reduced significantly after the membrane became saturated, except for two types of membrane bioreactors: B-TCSCM and B-TCSGOM. These are tubular ceramic-supported carbonized and graphene-oxide membrane bioreactors, respectively. This suggests that the non-modified ultrafiltration ceramic support (TCS) cannot generate the required stable biofilm for effective dye

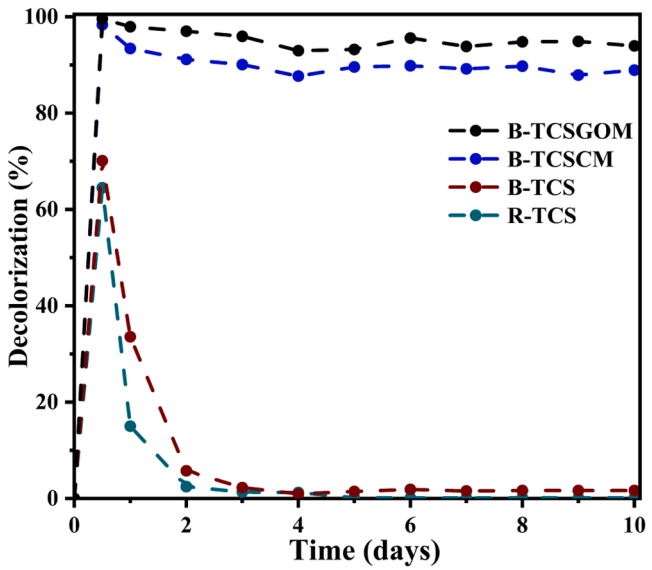

Fig. 7. Anaerobic decolorization of AO7 in TCS reactor and TCS, TCSCM, and TCSGOM bioreactors. Flux $= 0.10\ L{\cdot}m^{-2}{\cdot}h^{-1}$, $[AO7]_o = 50\ mg{\cdot}L^{-1}$ and T = 37 °C.

removal or filter out dye molecules from the feed solution, as the pores are comparatively larger than the dye molecules, to facilitate the pore-blocking filtration mechanism. Even though B-CS was operated with microorganisms, the intended biodecolorization did not happen because of the absence of an active biofilm. Like R-TCS, it is possible that the bacteria were washed out before a biofilm could form due to the small size of their cells compared to the pores in the support material. In turn, after three days of operation, the decolorization in the carbon-based membrane bioreactors remained highly stable throughout the experiments. It appears that the nanoporous carbon layer of both carbon-based membranes was well suited for the anaerobic decolorization process under these conditions. As elsewhere stated [31,32], these membranes perform a triple role: they support microorganisms to grow a biofilm, immobilize and retain the pollutants, and enhance electron transfer between bacteria and dye molecules under anaerobic conditions.

The degradation mechanism in this integrated anaerobic degradation of azo dyes comprises two steps: the bacteria initially use the substrate to produce electrons, which are subsequently transported to the dye molecules in order to break the azo bonds. The electron-generating bacteria adhere to the membrane and keep building the biofilm. Thus, the conductive carbon-based membranes accelerate electron transfer between microorganisms and azo dyes, enhancing degradation and dye removal efficiency. In the biodecolorization of azo dyes, it is essential to note that the π-conjugated structure in the tubular graphene oxide membrane plays a crucial role as an electron transfer intermediator or redox mediator [33]. As a result, the graphene layers are more conductive than the carbonized matrimid layer, resulting in a quicker electron shuttle mediator effect [34]. In addition, the TCSGOM is formed with hydroxyl, carbonyl, and epoxy groups at its base plane and carboxyl groups at its lateral edges, which provide strong absorbing affinity to azo dyes and allow the bacteria to immobilize at its large surface due to good biocompatibility [35].

Moreover, some of the electrons were accepted on the graphene oxide membrane surface. At this point, the microbial consortium turned the GO into rGO (reduced graphene oxide). After the azo dyes were broken down, the rGO turned into GO, and the cycle started again [36]. Thus, the enhanced microbial metabolism in TCSGOM provides a higher anaerobic decolorization than the others [37]. Contrary to findings in some previous research [38,39], graphene oxide has not shown a detrimental effect on bacteria, allowing biofilm growth and attachment over the membrane surface.

After each biodecolorization experiment, backflushing of Milli-Q water was conducted for 30 min at 2 bar to clean the membrane, which was able to remove any dye molecule adsorbed on either the carbonaceous layer or the ceramic support, as well as to wash out the biofilm from the membrane surface. This allowed the membrane to recover the initial permeate flux without any noticeable structural changes or loss caused by bioreduction activity. Thus, the used membrane can be utilized for future experiments.

3.4. TCSCM and TCSGOM performance for decolorization of azo dyes

The effect of feed concentration on the biodecolorization performance was investigated for the three structurally different azo dyes (monoazo AO7, diazo RB5, triazo DB71) using both B-TCSCM and B-TCSGOM. Three different feed solution concentrations were explored in the experiments: 50, 75, and 100 $mg{\cdot}L^{-1}$. In all cases, the bioreactors were operated under a constant permeate flux of 0.10 $L{\cdot}m^{-2}{\cdot}h^{-1}$, which was controlled by adjusting the TMP regularly.

Fig. 8(a-i) illustrates the extent of the color removal for the three dye solutions during a one-month operation. As expected, it can be seen that the decolorization depends on the feed concentration, the number of azo bonds, and, probably, the other functional groups present in the dye molecules. The decolorization performance was also significantly influenced by the type of carbonaceous layer. Logically, irrespective of the feed concentration, the monoazo AO7 gave the highest color removal, 92–97 % in TCSGOM and 75–90 % in TCSCM. Table 1 collects the dye removal and decolorization rate for the B-TCSCM and B-TCSGOM processes using the different feed concentrations and dyes. Notably, as feed concentration increases, decolorization decreases, but the hourly normalized amount of decolorized dye increases. Regardless of the membrane bioreactor, the maximum amount of dye removal (9.2 $mg{\cdot}m^{-2}{\cdot}h^{-1}$ for B-TCSGOM and 7.5 $mg{\cdot}m^{-2}{\cdot}h^{-1}$ for B-TCSCM) was obtained for 100 $mg{\cdot}L^{-1}$ of AO7, while DB71 at the same feed concentration gave the lowest 6.2 and 7.8 $mg{\cdot}m^{-2}{\cdot}h^{-1}$ for B-TCSCM and B-TCSGOM, respectively.

Overall, color removal was significantly higher and more stable in all experiments in the bioreactors operated with the tubular graphene oxide membrane. Under the same operating condition and feed solution, the reason for the superior performance of TCSGOM than TCSCM may be attributed to its superior conductive surface, which enhances the role of a redox mediator due to its better electron transfer capacity during biodegradation. This way, it boosts the quick electron transfer from the bacteria to the azo bonds, followed by breaking the azo bonds of dye molecules to give a colorless product [40]. Moreover, for any azo dye and feed concentrations applied, B-TCSGOM adapted very well to increasing concentration and removed color significantly better than TCSCM does. However, in both bioreactors, the biofilm was almost equally stable to give a consistent degradation rate and rapidly reactivated after each increase in feed concentration. Overall, the integrated system has a very robust operational performance.

There is evidence that the decolorization of azo dyes generally depends on the existence of one or more azo bonds connected to sulphonates, -OH and -NH_2 groups, and on the molecular weight of the dye molecule [41,42]. The triazo DB71 contains three azo bonds as well as more chromophores and auxochromes groups than AO7 and RB5. The increased presence of such reactive groups in the dye readily reduced microbial growth [43]. Additionally, compared to monoazo dye, the more significant toxicity in diazo and triazo molecules resulted in a decline of the decolorization effectiveness by ruining the biofilm or active sites of the microorganisms. This was also found in the present research work. Thus, Fig. 8(a-i) shows that the decolorization rate worsens (90–80 % for B-TCSCM and 97–88 % for B-TCSGOM) when the feed solution contains more azo, aromatic, and functional groups. Accordingly, for both bioreactors, the steady color removal followed the order: AO7 > RB5 > DB71. Franciscon et al. [44] and Amin et al. [16,17] previously observed that the monoazo dye removal was faster and

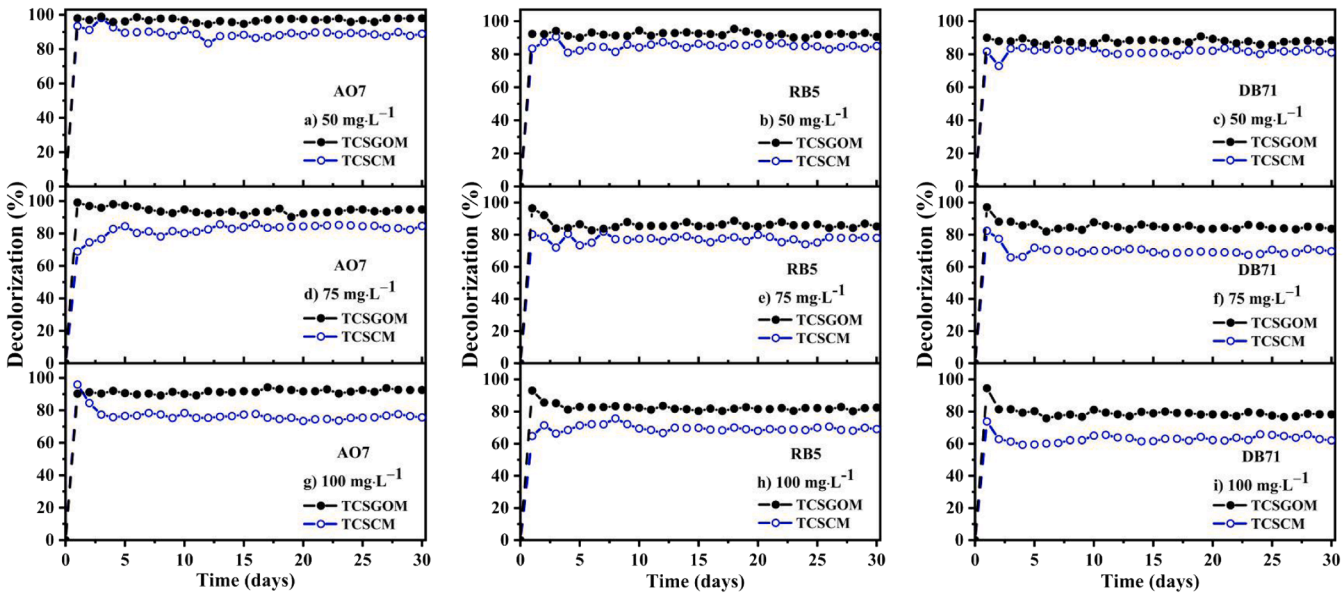

Fig. 8. Anaerobic decolorization of Acid Orange 7, Reactive Black 5, and Direct Blue 71 at 37 °C for various feed dye concentrations; a-c) 50 mg·L^{-1}, d-f) 75 mg·L^{-1} and g-i) 100 mg·L^{-1}. TCSCM: 10 % wt. of Matrimid and TCSGOM: 1 mg·mL^{-1} of GO.

Table 1
Summary of the decolorization and removal of azo dyes.

Dye	Concentration (mg·L^{-1})	B-TCSCM		B-TCSGOM	
		Decolorization (%)	Dye Removal Rate (mg·m^{-2}·h^{-1})	Decolorization (%)	Dye Removal Rate (mg·m^{-2}·h^{-1})
AO7	50	90	4.5	97	4.9
	75	84	6.3	94	7.1
	100	75	7.5	92	9.2
RB5	50	84	4.2	90	4.5
	75	77	5.8	85	6.4
	100	69	6.9	82	8.2
DB71	50	80	4.0	88	4.4
	75	69	5.2	84	6.3
	100	62	6.2	78	7.8

more efficient than diazo and triazo using anaerobic bacterial bioreduction processes, while a similar trend was also obtained by Garcia et al. [45] using the electro-Fenton method. Once again, it was evident that faster electron transport is crucial for the anaerobic decolorization of azo dye solutions.

As expected, the dye removal was better in the bioreactors operated at a low feed concentration. For instance, the adverse effect of a growing feed concentration on the dye removal of B-TCSGOM was followed (as shown in Fig. 8) by increasing the feed concentration first from 50 to 75 mg·L^{-1} and later up to 100 mg·L^{-1}. Hence, the decolorization for the AO7, the RB5, and the DB71 solutions declined from 97 % to 92 %, 90–82 %, and 88–78 %, respectively. A similar trend was obtained for B-TCSCM, where the reductions were as follows: 90–75 % for AO7, 84–69 % for RB5, and 80–62 % for DB71. It is well-known that a low feed concentration in the reactor system allows the dye molecules to interact more suitably with bacteria to reach significant biodegradation [46]. Under these circumstances, the biomass present was adequate to support almost complete bioreduction. On the other hand, increasing feed concentration in the bioreactors introduces a higher dye load with additional chromophores and auxochromes content in the anaerobic biodegradation pathways.

Therefore, excess amounts of these functional groups (-SO_3H, -R, -NH_2, -SO_2NH_2, etc.) severely reduce microbial growth in the reactors, consequently lessening the decolorization performance [47–49]. In addition, the toxic substances can limit the biomass load and microorganism tolerance, which lowers the decolorization rate, too.

This trend was already observed in our previous research, where the anaerobic decolorization of azo dyes was performed using flat ceramic-supported carbonized Matrimid and graphene oxide membrane bioreactors [16,17]. Using CSCM, the biodecolorization achieved in those experiments was 36–57 %, 30–42 %, and 26–34 % for AO7, RB5, and DB71, respectively. In comparison to the flat membrane bioreactor [16], TCSCM demonstrated about 33 %, 50 %, and 66 % greater dye removal rates for AO7, RB5, and DB7, respectively. The tubular bioreactor provides better coverage and roughness, where the surface area of the biofilm and the amount of biomass are increased; this contributed to improving the decolorization rate. However, comparing B-TCSGOM to B-CSGOM, i.e., tubular versus flat, except for the higher amount of filtered liquid, the percentage of color removal was almost identical [17]. On the other hand, the degree of decolorization declines as the feed concentration increases. However, the amount of dye removed increased steadily, and the highest dye removal in absolute terms was obtained with 100 mg·L^{-1} of each azo dye solution (Table 1).

4. Conclusions

To summarize, two tubular carbon-based membranes to be used in bioreactors were successfully prepared using a carbonized polymer precursor (TCSCM) or graphene oxide (TCSGOM) over a ceramic filtration element as support by means of easily scalable procedures. The

TCSGOM had a water permeance of 22.8 $L \cdot m^{-2} \cdot h^{-1} \cdot bar^{-1}$, showing that the GO membrane nanoporous surface was responsible for its lower permeance than the tubular support and TCSCM.

The overall performance of TCSCM and TCSGOM was evaluated with different types of azo dyes (mono-, di- and tri-azo dyes) and several feed concentrations. In all experiments, regardless of the type of azo dye and operating conditions, the TCSGOM bioreactor gave better color removal than the TCSCM. The highest biodecolorization using B-TCSGOM was 97 % for AO7, 94 % for RB5, and 92 % for DB71 at the lowest feed concentration; in turn, for B-TCSCM, it was 90 %, 84 %, and 80 %, respectively. Based on the research conducted, it has been found that the graphene oxide layer in the TCSGOM bioreactor has a superior electron transfer mechanism compared to the carbonaceous layer in the matrimid-based TCSCM bioreactor. Moreover, the GO layer at the nanoscale facilitates the formation of durable biofilms and improves the efficacy of retaining dye molecules and byproducts of biodegradation.

CRediT authorship contribution statement

Mohammad Shaiful Alam Amin: Conceptualization, Methodology, Investigation, Writing – original draft. **Frank Stüber:** Resources, Writing – review & editing. **Jaume Giralt:** Writing – review & editing. **Agustí Fortuny:** Validation, Writing – review & editing. **Azael Fabregat:** Validation, Writing – review & editing. **Josep Font:** Funding acquisition, Project administration, Conceptualization, Methodology, Supervision, Writing – review & editing.

Declaration of Competing Interest

The authors declare that they have no known competing financial interests or personal relationships that could have appeared to influence the work reported in this paper.

Data availability

Data will be made available on request.

Acknowledgements

This project has been supported by the European Union's Horizon 2020 Research and Innovation Programme under the Marie Skłodowska-Curie grant agreement No. 713679 and by the Universitat Rovira i Virgili (URV), contract 2017MFP-COFUND-18. This article was possible thanks to the grants RTI2018-096467-B-I00 and PID2021-126895OB-I00 funded by MCIN/AEI/ 10.13039/501100011033 and "ERDF A way of making Europe". The authors research group is recognized by the Comissionat per a Universitats i Recerca, DIUE de la Generalitat de Catalunya (2017 SGR 396 and 2021 SGR 00200), and supported by the Universitat Rovira i Virgili (2021PFR-URV-87).

References

[1] G.A. Ismail, H. Sakai, Review on effect of different type of dyes on advanced oxidation processes (AOPs) for textile color removal, Chemosphere (2021), 132906, https://doi.org/10.1016/j.chemosphere.2021.132906.
[2] K.-T. Chung, Azo dyes and human health: a review, J. Environ. Sci. Health, Part C 34 (2016) 233–261, https://doi.org/10.1080/10590501.2016.1236602.
[3] B. Senthil Rathi, P.Senthil Kumar, Sustainable approach on the biodegradation of azo dyes: a short review, Curr. Opin. Green Sustain. Chem. 33 (2022), 100578, https://doi.org/10.1016/j.cogsc.2021.100578.
[4] M. Solís, A. Solís, H.I. Pérez, N. Manjarrez, M. Flores, Microbial decolouration of azo dyes: a review, Process Biochem. 47 (2012) 1723–1748, https://doi.org/10.1016/j.procbio.2012.08.014.
[5] F. McYotto, Q. Wei, D.K. Macharia, M. Huang, C. Shen, C.W.K. Chow, Effect of dye structure on color removal efficiency by coagulation, Chem. Eng. J. 405 (2021), 126674, https://doi.org/10.1016/j.cej.2020.126674.
[6] C.Y. Teh, P.M. Budiman, K.P.Y. Shak, T.Y. Wu, Recent advancement of coagulation–flocculation and its application in wastewater treatment, Ind. Eng. Chem. Res. 55 (2016) 4363–4389, https://doi.org/10.1021/acs.iecr.5b04703.
[7] R. Andreozzi, V. Caprio, A. Insola, R. Marotta, Advanced oxidation processes (AOP) for water purification and recovery, Catal. Today 53 (1999) 51–59, https://doi.org/10.1016/S0920-5861(99)00102-9.
[8] H. Hansson, F. Kaczala, M. Marques, W. Hogland, Photo-Fenton and Fenton oxidation of recalcitrant industrial wastewater using nanoscale zero-valent iron, Int. J. Photoenergy 2012 (2012) 11, https://doi.org/10.1155/2012/531076.
[9] İ. Koyuncu, H. Afşar, Decomposition of dyes in the textile wastewater with ozone, J. Environ. Sci. Health Part A Environ. Sci. Eng. Toxicol. 31 (1996) 1035–1041, https://doi.org/10.1080/10934529609376405.
[10] M.J. Uddin, M.A. Islam, S.A. Haque, S. Hasan, M.S.A. Amin, M.M. Rahman, Preparation of nanostructured TiO2-based photocatalyst by controlling the calcining temperature and pH, Int. Nano Lett. 2 (2012) 1–10, https://doi.org/10.1186/2228-5326-2-19.
[11] M. Moreno-Benito, E. Yamal-Turbay, A. Espuña, M. Pérez-Moya, M. Graells, Optimal recipe design for Paracetamol degradation by advanced oxidation processes (AOPs) in a pilot plant, in: A. Kraslawski, I. Turunen (Eds.), Computer Aided Chemical Engineering, Elsevier, 2013, pp. 943–948, https://doi.org/10.1016/B978-0-444-63234-0.50158-5.
[12] V. Kumar, M.P. Shah, 1 - Advanced oxidation processes for complex wastewater treatment, in: M.P. Shah (Ed.), Advanced Oxidation Processes for Effluent Treatment Plants, Elsevier, 2021, pp. 1–31, https://doi.org/10.1016/B978-0-12-821011-6.00001-3.
[13] M. Islam, M. Amin, J. Hoinkis, Optimal design of an activated sludge plant: theoretical analysis, Appl. Water Sci. 3 (2013) 375–386, https://doi.org/10.1007/s13201-013-0088-z.
[14] Y. García-Martínez, J. Chirinos, C. Bengoa, F. Stüber, J. Font, A. Fortuny, A. Fabregat, Fast aqueous biodegradation of highly-volatile organic compounds in a novel anaerobic reaction setup, Environments 5 (2018) 115, https://doi.org/10.3390/environments5110115.
[15] E. Obotey Ezugbe, S. Rathilal, Membrane technologies in wastewater treatment: a review, Membranes 10 (2020) 89, https://doi.org/10.3390/membranes10050089.
[16] M.S.A. Amin, F. Stüber, J. Giralt, A. Fortuny, A. Fabregat, J. Font, Comparative anaerobic decolorization of Azo dyes by carbon-based membrane bioreactor, Water 13 (2021) 1060, https://doi.org/10.3390/membranes12020174.
[17] M.S.A. Amin, F. Stüber, J. Giralt, A. Fortuny, A. Fabregat, J. Font, Ceramic-supported graphene oxide membrane bioreactor for the anaerobic decolorization of azo dyes, J. Water Process Eng. 45 (2022), 102499, https://doi.org/10.1016/j.jwpe.2021.102499.
[18] M.S.A. Amin, F. Stüber, J. Giralt, A. Fortuny, A. Fabregat, J. Font, Compact carbon-based membrane reactors for the intensified anaerobic decolorization of dye effluents, Membranes 12 (2022) 174, https://doi.org/10.3390/membranes12020174.
[19] M.S.A. Amin, M.S.I. Mozumder, F. Stüber, J. Giralt, A. Fortuny, A. Fabregat, J. Font, Biofilm model development and process analysis of anaerobic bio-digestion of azo dyes, Environ. Technol. Innov. 29 (2023), 102962, https://doi.org/10.1016/j.eti.2022.102962.
[20] A. Giménez-Pérez, S.K. Bikkarolla, J. Benson, C. Bengoa, F. Stüber, A. Fortuny, A. Fabregat, J. Font, P. Papakonstantinou, Synthesis of N-doped and non-doped partially oxidised graphene membranes supported over ceramic materials, J. Mater. Sci. 51 (2016) 8346–8360, https://doi.org/10.1007/s10853-016-0075-5.
[21] F.P. van der Zee, S. Villaverde, Combined anaerobic–aerobic treatment of azo dyes—A short review of bioreactor studies, Water Res. 39 (2005) 1425–1440, https://doi.org/10.1016/j.watres.2005.03.007.
[22] N.D. Lourenço, J.M. Novais, H.M. Pinheiro, Effect of some operational parameters on textile dye biodegradation in a sequential batch reactor, J. Biotechnol. 89 (2001) 163–174, https://doi.org/10.1016/S0168-1656(01)00313-3.
[23] M.S. Khehra, H.S. Saini, D.K. Sharma, B.S. Chadha, S.S. Chimni, Decolorization of various azo dyes by bacterial consortium, Dyes Pigments 67 (2005) 55–61, https://doi.org/10.1016/j.dyepig.2004.10.008.
[24] M. El Bouraie, W.S.El Din, Biodegradation of Reactive Black 5 by Aeromonas hydrophila strain isolated from dye-contaminated textile wastewater, Sustain. Environ. Res. 26 (2016) 209–216, https://doi.org/10.1016/j.serj.2016.04.014.
[25] M.F. Elshahawy, G.A. Mahmoud, A.I. Raafat, A.E.-H. Ali, Es.A. Soliman, Fabrication of TiO_2 reduced graphene oxide based nanocomposites for effective of photocatalytic decolorization of dye effluent, J. Inorg. Organomet. Polym. Mater. 30 (2020) 2720–2735, https://doi.org/10.1007/s10904-020-01463-3.
[26] N. Sazali, W.N.W. Salleh, N.A.H. Md Nordin, Z. Harun, A.F. Ismail, Matrimid-based carbon tubular membranes: the effect of the polymer composition, J. Appl. Polym. Sci. 132 (2015) 1–12, https://doi.org/10.1002/app.42394.
[27] J.N. Barsema, S.D. Klijnstra, J.H. Balster, N.F.A. van der Vegt, G.H. Koops, M. Wessling, Intermediate polymer to carbon gas separation membranes based on Matrimid PI, J. Membr. Sci. 238 (2004) 93–102, https://doi.org/10.1016/j.memsci.2004.03.024.
[28] N.H. Ismail, W.N.W. Salleh, N. Sazali, A.F. Ismail, N. Yusof, F. Aziz, Disk supported carbon membrane via spray coating method: effect of carbonization temperature and atmosphere, Sep. Purif. Technol. 195 (2018) 295–304, https://doi.org/10.1016/j.seppur.2017.12.032.
[29] N. Sazali, W.N.W. Salleh, N.A.H.M. Nordin, A.F. Ismail, Matrimid-based carbon tubular membrane: effect of carbonization environment, J. Ind. Eng. Chem. 32 (2015) 167–171, https://doi.org/10.1016/j.jiec.2015.08.014.
[30] N.H. Ismail, W.N.W. Salleh, N. Sazali, A.F. Ismail, Effect of intermediate layer on gas separation performance of disk supported carbon membrane, Sep. Sci. Technol. 52 (2017) 2137–2149, https://doi.org/10.1080/01496395.2017.1321671.
[31] G. Mezohegyi, C. Bengoa, F. Stuber, J. Font, A. Fabregat, A. Fortuny, Novel bioreactor design for decolourisation of azo dye effluents, Chem. Eng. J. 143 (2008) 293–298, https://doi.org/10.1016/j.cej.2008.05.006.

[32] J. Ming, D. Sun, J. Wei, X. Chen, N. Zheng, Adhesion of bacteria to a graphene oxide film, ACS Appl. Bio Mater. 3 (2020) 704–712, https://doi.org/10.1021/acsabm.9b01028.
[33] J. Shen, M. Shi, B. Yan, H. Ma, N. Li, Y. Hu, M. Ye, Covalent attaching protein to graphene oxide via diimide-activated amidation, Colloids Surf. B Biointerfaces 81 (2010) 434–438, https://doi.org/10.1016/j.colsurfb.2010.07.035.
[34] J. Ma, D. Ping, X. Dong, Recent developments of graphene oxide-based membranes: a review, Membranes 7 (2017), https://doi.org/10.3390/membranes7030052.
[35] G. Wang, F. Qian, C.W. Saltikov, Y. Jiao, Y. Li, Microbial reduction of graphene oxide by Shewanella, Nano Res. 4 (2011) 563–570, https://doi.org/10.1007/s12274-011-0112-2.
[36] Z. Li, J. Zhao, B. Liu, L. Yang, G. Han, F. Yang, S. Han, Z. Wang, Z. Zhang, Graphene oxide composite membrane accelerates organic pollutant degradation by Shewanella bacteria, Water Sci. Technol. 84 (2021) 1037–1047, https://doi.org/10.2166/wst.2021.285.
[37] Y. García-Martínez, C. Bengoa, F. Stüber, A. Fortuny, J. Font, A. Fabregat, Biodegradation of acid orange 7 in an anaerobic–aerobic sequential treatment system, Chem. Eng. Process. Process. Intensif. 94 (2015) 99–104, https://doi.org/10.1016/j.cep.2014.12.011.
[38] V.R.S.S. Mokkapati, S. Pandit, J. Kim, A. Martensson, M. Lovmar, F. Westerlund, I. Mijakovic, Bacterial response to graphene oxide and reduced graphene oxide integrated in agar plates, R. Soc. Open Sci., 5 181083. https://doi.org/https://doi.org/10.1098/rsos.181083.
[39] P.-C. Wu, H.-H. Chen, S.-Y. Chen, W.-L. Wang, K.-L. Yang, C.-H. Huang, H.-F. Kao, J.-C. Chang, C.-L.L. Hsu, J.-Y. Wang, T.-M. Chou, W.-S. Kuo, Graphene oxide conjugated with polymers: a study of culture condition to determine whether a bacterial growth stimulant or an antimicrobial agent? J. Nanobiotechnol. 16 (2018) 1, https://doi.org/10.1186/s12951-017-0328-8.
[40] X. Xiao, T.-T. Li, X.-R. Lu, X.-L. Feng, X. Han, W.-W. Li, Q. Li, H.-Q. Yu, A simple method for assaying anaerobic biodegradation of dyes, Bioresour. Technol. 251 (2018) 204–209, https://doi.org/10.1016/j.biortech.2017.12.052.
[41] M. Berradi, R. Hsissou, M. Khudhair, M. Assouag, O. Cherkaoui, A. El Bachiri, A. El Harfi, Textile finishing dyes and their impact on aquatic environs, Heliyon 5 (2019), e02711, https://doi.org/10.1016/j.heliyon.2019.e02711.
[42] R. Khan, P. Bhawana, M.H. Fulekar, Microbial decolorization and degradation of synthetic dyes: a review, Rev. Environ. Sci. Bio/Technol. 12 (2013) 75–97, https://doi.org/10.1007/s11157-012-9287-6.
[43] Y. Shi, Z. Yang, L. Xing, X. Zhang, X. Li, D. Zhang, Recent advances in the biodegradation of azo dyes, World J. Microbiol. Biotechnol. 37 (2021) 137, https://doi.org/10.1007/s11274-021-03110-6.
[44] E. Franciscon, A. Zille, F. Fantinatti-Garboggini, I.S. Silva, A. Cavaco-Paulo, L. R. Durrant, Microaerophilic–aerobic sequential decolourization/biodegradation of textile azo dyes by a facultative Klebsiella sp. strain VN-31, Process Biochem. 44 (2009) 446–452, https://doi.org/10.1016/j.procbio.2008.12.009.
[45] S. Garcia-Segura, F. Centellas, C. Arias, J.A. Garrido, R.M. Rodríguez, P.L. Cabot, E. Brillas, Comparative decolorization of monoazo, diazo and triazo dyes by electro-Fenton process, Electrochim. Acta 58 (2011) 303–311, https://doi.org/10.1016/j.electacta.2011.09.049.
[46] M. Rahimi, B. Aghel, M. Sadeghi, M. Ahmadi, Using Y-shaped microreactor for continuous decolorization of an Azo dye, Desalin. Water Treat. 52 (2014) 5513–5519, https://doi.org/10.1080/19443994.2013.807471.
[47] B.-Y. Chen, Understanding decolorization characteristics of reactive azo dyes by Pseudomonas luteola: toxicity and kinetics, Process Biochem. 38 (2002) 437–446, https://doi.org/10.1016/S0032-9592(02)00151-6.
[48] S. Popli, U.D. Patel, Destruction of azo dyes by anaerobic–aerobic sequential biological treatment: a review, Int. J. Environ. Sci. Technol. 12 (2015) 405–420, https://doi.org/10.1007/s13762-014-0499-x.
[49] B.-Y. Chen, S.-Y. Chen, J.-S. Chang, Immobilized cell fixed-bed bioreactor for wastewater decolorization, Process Biochem. 40 (2005) 3434–3440, https://doi.org/10.1016/j.procbio.2005.04.002.